

The case for energy harvesting on wildlife in flight

This content has been downloaded from IOPscience. Please scroll down to see the full text.

2015 Smart Mater. Struct. 24 025031

(<http://iopscience.iop.org/0964-1726/24/2/025031>)

View [the table of contents for this issue](#), or go to the [journal homepage](#) for more

Download details:

IP Address: 128.253.224.105

This content was downloaded on 03/02/2015 at 19:06

Please note that [terms and conditions apply](#).

The case for energy harvesting on wildlife in flight

Michael W Shafer¹, Robert MacCurdy², J Ryan Shipley³, David Winkler³, Christopher G Guglielmo⁴ and Ephraim Garcia^{2,5}

¹ Department of Mechanical Engineering, Northern Arizona University, Flagstaff, AZ 86011, USA

² Sibley School of Mechanical and Aerospace Engineering, Cornell University, Ithaca, NY 14850, USA

³ Department of Ecology and Evolutionary Biology, Cornell University, Ithaca, NY, USA

⁴ Department of Biology, Advanced Facility for Avian Research, University of Western Ontario, London, ON, Canada

E-mail: michael.shafer@nau.edu

Received 27 August 2014, revised 20 November 2014

Accepted for publication 24 November 2014

Published 23 January 2015



CrossMark

Abstract

The confluence of advancements in microelectronic components and vibrational energy harvesting has opened the possibility of remote sensor units powered solely from the motion of their hosts. There are numerous applications of such systems, including the development of modern wildlife tracking/data-logging devices. These 'bio-logging' devices are typically mass-constrained because they must be carried by an animal. Thus, they have historically traded scientific capability for operational longevity due to restrictions on battery size. Recently, the precipitous decrease in the power requirements of microelectronics has been accompanied by advancements in the area of piezoelectric vibrational energy harvesting. These energy harvesting devices are now capable of powering the type of microelectronic circuits used in bio-logging devices. In this paper we consider the feasibility of employing these vibrational energy harvesters on flying vertebrates for the purpose of powering a bio-logging device. We show that the excess energy available from birds and bats could be harvested without adversely affecting their overall energy budget. We then present acceleration measurements taken on flying birds in a flight tunnel to understand modulation of flapping frequency during steady flight. Finally, we use a recently developed method of estimating the maximum power output from a piezoelectric energy harvester to determine the amount of power that could be practically harvested from a flying bird. The results of this analysis show that the average power output of a piezoelectric energy harvester mounted to a bird or bat could produce more than enough power to run a bio-logging device. We compare the power harvesting capabilities to the energy requirements of an example system and conclude that vibrational energy harvesting on flying birds and bats is viable and warrants further study, including testing.

Keywords: avian, bat, bio-logger, piezoelectric, energy harvesting

1. Introduction

Battery life is a limiting factor for wildlife tracking and bio-logging devices. For long deployments, even modern devices have a large portion of their mass dedicated to batteries. This has driven a need for *in situ* energy generation, recognized as

far back as 1973 [1]. Solar-powered bird tags with masses as low as 5 g now exist [2], yet are not universally applicable. Microwave Telemetry Inc, a wildlife tag manufacturer, offers solar-powered tags, yet their website notes preening habits or extensive time spent in shade preclude their use for many species [3]. In this work we consider how an animal's kinetic energy can be converted to electrical energy in order to power biological monitoring tags. The application of this method of energy conversion, known as vibrational energy harvesting, to bio-loggers was originally conceived for birds and moths [4]. It

⁵ This paper is dedicated to the memory of E Garcia, who sadly passed away prior to publication. His innovative ideas and engaging personality will be keenly missed by all who knew him.

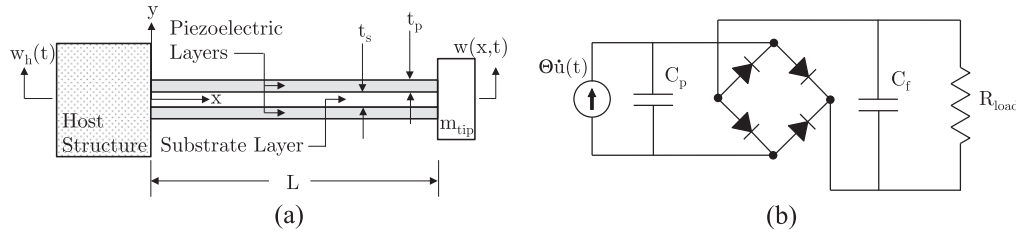


Figure 1. (a) Piezoelectric energy harvester. (b) Typical energy harvester circuit model. Piezoelectric harvesters modeled as current source in parallel with a capacitor.

could be applied to a wide variety of animals, but we focus here on flying vertebrates. We will show that when applied on birds or bats, where system mass is limited due to the constraints of flight, sufficient power is available to warrant use.

Vibrational energy harvesting is a method of converting mechanical energy to electrical energy. Piezoelectric devices are an ideal candidate for wildlife energy harvesting due to mechanical simplicity and high output voltage. Piezoelectric materials develop electric fields when under stress. Connecting a harvesting circuit to these materials allows the energy from an applied stress to be transduced for charging batteries or capacitors. While work continues on advanced designs, a standard cantilevered piezoelectric harvester and associated energy harvesting circuit are shown in figure 1. When excited, the strain induced in the beam from vibration is converted to electrical energy by the piezoelectric material. The current that develops in the harvesting circuit is rectified and converted to DC using a filtering capacitor. The circuit powered by the harvesters is often modeled as a resistive load. It is particularly important that these devices be excited at their resonant frequency, as power decreases when off-resonance [5, 6]. Here we will show the compatibility of this excitation requirement with the acceleration measurements from two bird species.

Vibrational energy harvesting has been demonstrated on small animals such as tobacco hornworm moths (*Manduca sexta*) and green June beetles (*Cotinis nitida*) [7, 8]. With their cyclic flapping gate, flying animals are an ideal candidate for vibrational energy harvesting. For instance, over a wide range of flight speeds, the flapping frequency of cockatiels (*Nymphicus hollandicus*) does not change by more than 20% [9]. A similar pattern exists in bats where stroke amplitude (not frequency) modulates flight speed [10].

To assess the viability of energy harvesting for this application, we first investigate the energy available. A method for this estimation developed by Shafer and Garcia [11], is reviewed and refined here with updated coefficients. It estimates a ceiling of what the animal is capable of supplying without adverse effects. We look at the energy output from flying birds and bats, and develop limits on the power that might be harvested in consideration of the animal's energy budget. We then present an analysis of acceleration measurements from two species of birds. Here we further analyze the testing results preliminarily presented by Shafer *et al* [12] to understand frequency consistency in relation to that required by energy harvesters. We then use estimates for the power limits of piezoelectric energy harvesters to predict the

capabilities of devices scaled for birds and bats. These power results are contrasted against the requirements of commercially available microcontrollers to show that more power can be generated than is required for device operation.

2. Energy harvesting limits and potential for animals in powered flight

The energy available for harvesting from an animal is related to their energy expenditure. For flying vertebrates, the power required for flight can be calculated from parameters such as wing aspect ratio, wing span, and mass. By subtracting the power required for flight for an unladen animal from that required by a laden animal, we develop an estimate of the animal's excess power capabilities. We use Pennycuik's flight model here due to its continued refinement [13–15]. The details of this model are presented in appendix A. Pennycuik's model originally developed for birds is remarkably similar to the scaling results when applied to bats [16], and provides the basis in our application for estimating harvestable power in bats. Although newer bat-specific flight models have been developed, the Pennycuik model is justified here as its estimates are conservative for harvestable power [10]. In this power model, the energy expenditure is decomposed into five major categories (parasitic, induced, profile, basal metabolic, and cardio/pulmonary). Descriptions and equations for each of these types of power are shown in tables A1 and A2. By calculating the power required for flight with and without a payload, we are able to make an estimate of available excess energy and assume this to be the power available for harvest.

Birds and bats are capable of flying for short periods with significant payloads. Marden experimentally showed that bird species are able to take off with payloads of 16% of their flight muscle mass [17]. This corresponds to about 5% of total body mass, assuming flight muscles are 25–35% of total mass. Traditionally devices attached to flying vertebrates have been limited by mass. Although new research suggests that energy output might be an alternate metric [18], the mass limit suggested by the US Geological Survey for migratory bird tags is 3% of the bird's mass [19] and 5% has been suggested for bats [20]. Others have proposed values in the range of 3–5% [21]. Research suggests 5% may be conservative for small birds and excessive for large birds [22]. Naef-Daenzner *et al* showed that the coal tit and great tit (*Parus ater* and *Parus major*) could carry payloads of 3–5% of their mass

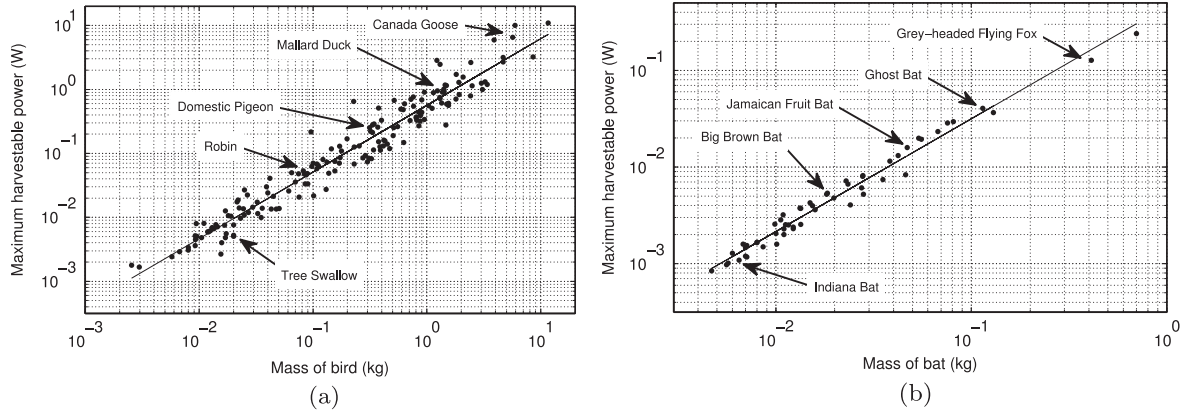


Figure 2. Maximum harvestable power (P_H) assuming 4% laden mass limit for birds (a) and bats (b).

without effects on survivability [23]. A similar pattern emerges in bats. Lesser horseshoe bats (*Rhinolophus hipposideros*) carrying 4.5–8.1% and big brown bats (*Eptesicus fuscus*) carrying 5% showed no effects on survivability [20, 24]. Taken together this suggests that for birds and bats the increased energy output required to carry a 4% payload would be tolerated well and could serve as a conservative estimate of the harvestable energy.

With a payload limit of 4% of the animal's mass and a model for power in flight, we can determine the power that could be safely harvested. The total power required for flight by an unladen animal would be [25]

$$P = 1.1(P_{\text{par}} + P_{\text{ind}} + P_{\text{pro}} + R_M). \quad (1)$$

Note that the 1.1 factor is included to account for the cardio/pulmonary power. We denote the fraction of the animal's unladen mass (m) attributed to payload as 'q' such that

$$m_1 = q m. \quad (2)$$

The laden mass term (m_1) can be summed with the unladen mass (m) and the resulting total flown mass used in the expressions for power (appendix A). After simplifying, the power required for flight with a payload is [11]:

$$P = 1.1 \left[P_{\text{par}} + (1 + q)^2 P_{\text{ind}} + (1 + q)^{3/2} P_{\text{pro}} + R_M \right]. \quad (3)$$

Taking the difference between equations (3) and (1), and using the maximum allowable ($q_{\text{max}} = 4\%$) as the laden mass fraction, gives an estimate of the excess long-term power output. We designate this as the *maximum harvestable power*, P_H .

$$P_H = 1.1 \left[\left((1 + q_{\text{max}})^2 - 1 \right) P_{\text{ind}} + \left((1 + q_{\text{max}})^{3/2} - 1 \right) P_{\text{pro}} \right]. \quad (4)$$

The induced power and profile power terms are a function of the wing span, aspect ratio, and mass (see appendix A). Measurements of these parameters are available for a variety of species, allowing us to develop a general estimate of the harvestable power from flying vertebrates.

2.1. Harvestable power across species

With a maximum harvestable power expression (equation (4)) and an upper limit of payload ($q_{\text{max}} = 4\%$), we can calculate the sustainably harvestable power for any species for which we have sufficient data. Poole provides a list of wing areas and weights for 149 North American birds [26]. Although Poole does not report wingspan, we can interpolate span based on mass using the Cornell Lab of Ornithology database [27]. Thus birds not in the Cornell dataset were excluded. In addition to this dataset, Pennycuik provides wing area and span for 36 other species for a total of 169 birds. For bats, several recent research papers have provided similar measurements for 59 species from eight different families [10, 16].

The induced power (P_{ind}) depends on the flight speed of the animal. Birds tend to prefer to fly at that speed which minimizes total power output (V_{mp}) [28]. It is assumed the same is true for bats.

$$V_{\text{mp}} = \frac{0.76k^{1/4}(mg)^{1/2}}{\rho^{1/2}(S_b C_{\text{Db}} S_d)^{1/4}}. \quad (5)$$

This flight speed depends on the animal's mass (m), gravitational acceleration (g), air density (ρ), frontal body area (S_b), circular area swept by the wings (S_d), and two coefficients (C_{Db} and k). The body drag coefficient (C_{Db}) is typically set to a value of 0.1 [25, 29]. A value of 0.9 for the empirical induced drag factor (k) has been recently shown to better predict V_{mp} than the previous value of 1.2 [29]. We calculate V_{mp} for each of the animals in the dataset, and in conjunction with equation (4), we develop a harvestable power estimate across species. The results of this analysis are shown in figure 2.

Figure 2 provides an estimate of the power available across a large number of species of both birds (2(a)) and bats (2(b)). As shown in the figure, the power has a power-law relationship with the mass of the animal. A regression analysis provides the relationship between mass and harvestable power. The results are plotted in figure 2 with the relationships being:

$$P_{H_{\text{bird}}} = 0.565m^{1.043}, \quad (6)$$

$$R_{\text{Hbat}} = 0.461m^{1.166}. \quad (7)$$

This is an initial estimate of the *total* excess power output capabilities of a flying animal and includes the power required to carry the system and power to be harvested. The power of the mass term in these relationships is near unity. This could allow future studies to use a simplified, yet less precise linear relationship between harvestable power and mass. Using the specific power of the transducer, we can account for the power required to carry the harvesting device, and obtain a more precise estimate of the power that could be harvested.

To account for the energy required to carry the harvester and payload, we distinguish between the power *required* for flight (P_r) and the maximum *allowable* output power (P_a). The power required for flight is simply the result of equation (3), where the total flown mass is used to calculate the induced and profile powers. This total flown mass is the sum of the masses of the animal, harvester, and any additional payload such as electronics, batteries, etc. The maximum allowable power output is expressed by equation (3), using the 4% laden mass limit (q_{max}). The required and the allowable powers can be expressed as follows:

$$P_r = 1.1(P_{\text{par}} + (1+q)^2 P_{\text{ind}} + (1+q)^{3/2} P_{\text{pro}} + R_M), \quad (8)$$

$$P_a = 1.1\left(P_{\text{par}} + (1+q_{\text{max}})^2 P_{\text{ind}} + (1+q_{\text{max}})^{3/2} P_{\text{pro}} + R_M\right). \quad (9)$$

The difference of these expressions is

$$P_h = 1.1\left[\left[(1+q_{\text{max}})^2 - (1+q)^2\right]P_{\text{ind}} + \left[(1+q_{\text{max}})^{3/2} - (1+q)^{3/2}\right]P_{\text{pro}}\right]. \quad (10)$$

Notice that we distinguish this *practically harvestable power* (P_h), which accounts for the mass of the payload and harvester, from the theoretically harvestable power (P_H), which depends only on q_{max} . When calculating this practically harvestable power, the P_{ind} and P_{pro} terms are calculated for the unladen animal, with the q term indicating the fraction of the total flown mass beyond the unladen mass. If we assume that the energy harvester has some specific power (\bar{P} , power per unit mass), then the total laden mass depends on the amount of available power. Introducing this dependency insures the harvester is appropriately sized for the power available for harvest. A harvester with specific power \bar{P} sized to harvest power P_h would have a mass P_h/\bar{P} . Adding to this a mass for payload components (m_p) like electronics, batteries, etc, (those not included in the harvester), the total laden mass of the system would be:

$$m_l = m_p + \frac{P_h}{\bar{P}}. \quad (11)$$

This expression can be used with equation (2) to solve for the laden mass fraction (q) in terms of the specific power, the harvestable power, and the payload mass. Substituting this result into equation (10) and rearranging results in the

following polynomial expression:

$$At^4 + Bt^3 + Ct^2 + E = 0, \quad (12)$$

$$t = \sqrt{P_h/\bar{P} + m + m_p}, \quad (13)$$

where

$$A = 1.1P_{\text{ind}}/m^2, \quad (14)$$

$$B = 1.1P_{\text{pro}}/m^{3/2}, \quad (15)$$

$$C = \bar{P}, \quad (16)$$

$$E = -1.1(1+q_{\text{max}})^2 P_{\text{ind}} - 1.1(1+q_{\text{max}})^{3/2} P_{\text{pro}} - \bar{P}(m+m_p). \quad (17)$$

This expression (equation (12)) has the following closed form solution for the practically harvestable power P_h :

$$P_h = \bar{P}(t^2 - m - m_p), \quad (18)$$

where

$$t = \frac{-B}{4A} + \frac{\pm_i W \mp_j \sqrt{-(3\lambda + 2y \pm \frac{2\beta}{iW})}}{2}. \quad (19)$$

The terms W , λ , y , and β are all components of the solution that depend on A , B , C , and E and are shown in appendix B. The i subscripts for the ' \pm ' signs indicate that they change sign independently of the j subscript on the ' \mp ' sign. With this solution we are able to estimate the practically harvestable power from an animal.

To make the estimate of practically harvestable power using equation (18), we use the same datasets used in estimating P_H . We make this estimate for a range of species and transducer specific powers. In figure 3(a) for birds and 3(b) for bats, we see contour lines of harvestable power plotted against transducer-specific power and animal mass. The peaks in the contour lines are a result of the fact that some species are more efficient fliers. These peaks appear smaller as the harvestable power decreases because of the linear contour scaling.

Generally, there is a dependence of the harvestable power on mass that can be seen in figure 3. The range of transducer specific power was selected to extend above and below the expected specific power of piezoelectric energy harvesters. A harvester sized to weigh a few grams and operate at approximately 10 Hz would expect a specific power of less than 0.5 W kg^{-1} [30]. We can see in figure 3 that a transducer with a specific power of $0.05\text{--}0.5 \text{ W kg}^{-1}$ may safely harvest $20\text{--}200 \mu\text{W}$ for the smallest of birds ($\mathcal{O}(10 \text{ g})$) and $20\text{--}200 \text{ mW}$ for the largest of birds ($\mathcal{O}(10 \text{ kg})$). Even for smaller birds, these results are sufficient to power a variety of microcontrollers that might be used on a bio-logging tag. Similar results occur for bats. While many microcontrollers operate with power requirements of a few milliwatts, some modern units employing FRAM are able to operate at speeds of 1 MHz using only $180 \mu\text{W}$ [31], well within the range of what could be harvested.

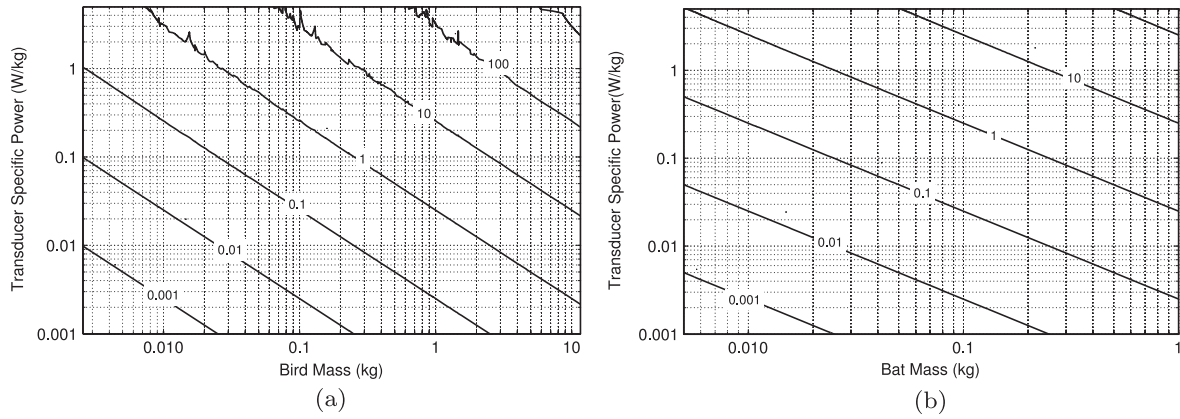


Figure 3. Practically harvestable power in milliwatts for birds (a) and bats (b) accounting for power to fly transducer.

3. Acceleration measurements on freely flying birds

3.1. Flight test overview

After determining the available energy from the host animal, here we determine the compatibility of the transducer technology with the animal's kinetics. As previously mentioned, resonant-type vibrational energy harvesters require a consistent excitation frequency for maximum power harvesting and evidence suggests that birds have a preferred flapping frequency across a range of flight speeds [9]. Additionally, there is evidence that birds consistently fly near the minimum power velocity [28]. This suggests that we might expect a uniform fundamental flapping frequency over long periods. Here we investigate flight motion frequency modulation of birds over short time scales to assess the compatibility with vibrational energy harvesting.

We conducted a series of tests on two bird species in a flight tunnel at the Advanced Facility for Avian Research at the University of Western Ontario. The test section of this tunnel is 2 m long, with a cross section 1 m high and 1.5 m wide [32]. The birds were outfitted with data-logging devices that measured three orthogonal components of acceleration at 200 Hz for 50 s. The data loggers consisted of a Texas Instruments MSP430F2274 microcontroller and a Bosch BMA150 3-axis accelerometer. The acceleration measurements were stored in local memory until they could be offloaded after each test. The devices weighed 0.44 g and can be seen in the figure 4 insert. The data loggers were held in place using a plastic harness (0.23 g) temporarily glued or tied using Rappole-style leg loops to the bird (see figure 4) [33]. When glued, feathers beneath the loggers were trimmed to ensure a more rigid connection. The harnesses allowed for easy removal of logging devices after each trial for data offload, and quick replacement for the next trial.

The two species of birds tested with these acceleration loggers were the western sandpiper (*Calidris mauri*) and the Swainson's thrush (*Catharus ustulatus*). One western sandpiper (WS) was flown and weighed 30.1 g. The two tested Swainson's thrushes weighed 40.8 g (ST1) and 41.0 g (ST2). These birds were captured under a Canadian Wildlife



Figure 4. Accelerometer tag mounted to sandpiper and tag with US dime for scale (insert).

Service permit (CA-0256) and experimental procedures were approved by the University of Western Ontario Animal Use Subcommittee (Protocol 2010-216). The thrushes tended to perform better in the tunnel, thus providing more data than did the sandpiper. The procedure for the tests was as follows: prior to testing, the birds were outfitted with the plastic harnesses. They were returned to their enclosures to become accustomed to the apparatus. At the beginning of each trial an acceleration logging device was inserted into the harness. The tunnel was brought up to 10 m s^{-1} equivalent wind speed (previously shown to be an appropriate speed for these birds [32]). The logging device was then turned on and the bird was released into the tunnel. The bird then flew in the tunnel until the memory on the logger was full (50 s) or the bird landed. When the bird landed before 50 seconds had elapsed, it was either prompted to fly again or recaptured to begin another test.

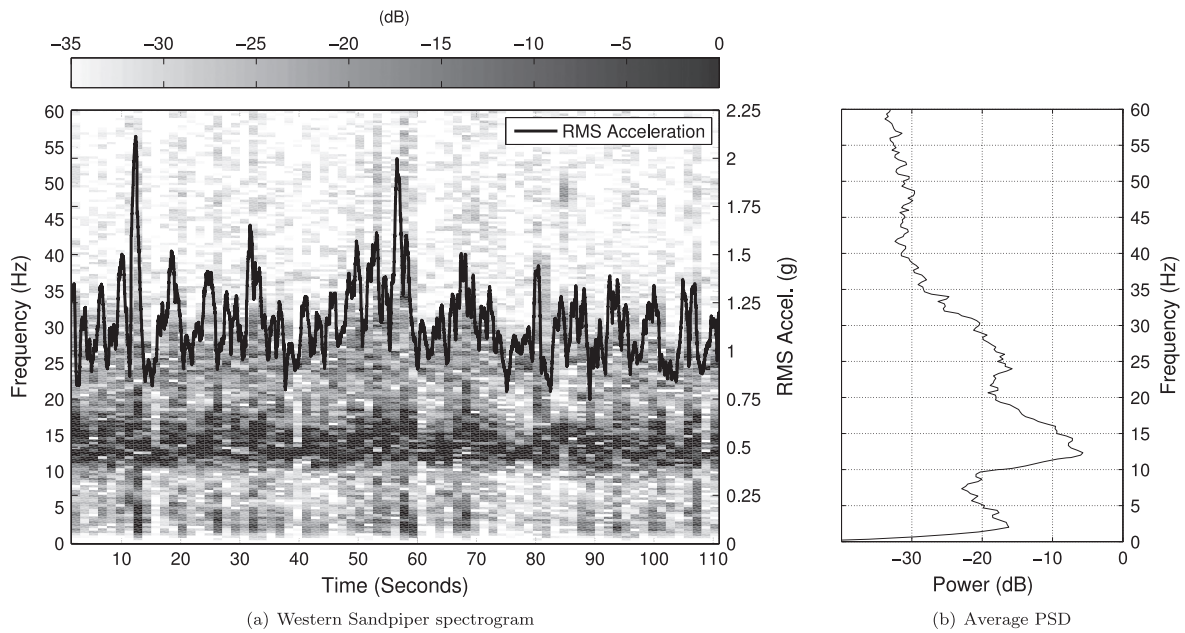


Figure 5. Spectral results of z-component acceleration for sandpiper trials. Notice relatively consistent frequency near 12 Hz. Sliding window (1 s) RMS acceleration magnitude plotted on second axis of spectrogram.

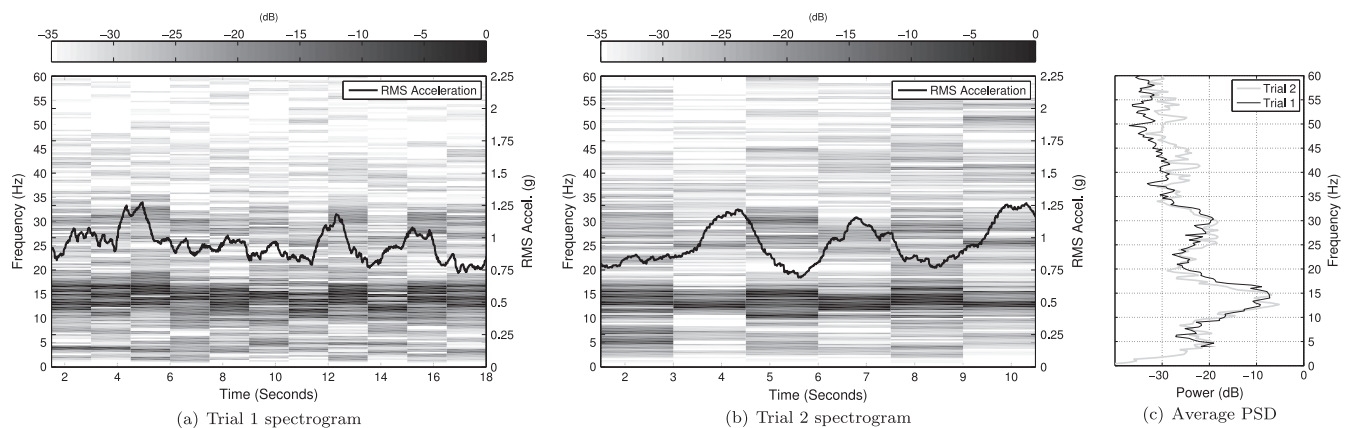


Figure 6. Spectral results of z-component acceleration for thrush 1. Two trials shown highlighting small shifts in flapping frequency from 12 Hz. Sliding window (1 s) RMS acceleration magnitude plotted on second axis of spectrogram.

3.2. Results

The trials from this testing have been grouped to highlight different aspects of the flight acceleration spectrum. The first group of results consists of three trials from sandpiper flights. These trials all have similar frequency content and show the consistency of flapping frequency in time. The second group consists of two trials from ST1, showing that there can be small fluctuations in the primary flapping frequency for a given species, but there is overlap in the average power spectral density peaks to allow for a single targeted resonance. The third group consists of four trials from ST2 highlighting the small effects of payload on the flapping frequency. We focus our analysis on the z-component of acceleration, pointing up off of the back of the bird. The 3-axis accelerometer results showed this direction containing the highest amplitude acceleration and would thus be the candidate for energy harvester excitation. Spectrograms of the results for each of the three groups are shown in figures 5–7.

These spectrograms result from dividing the acceleration signals into a series of discrete windows and performing a short-time Fourier analysis on each window. A 3 s Hamming window with 50% overlap was used, representing approximately 36 flapping cycles per window. Overlaid on these spectrograms is the moving RMS magnitude of the acceleration. The moving RMS is calculated using a one second sliding window. It should be noted that the acceleration signal has been highpass filtered with a 2 Hz cutoff frequency to eliminate the DC gravitational component. Thus, the RMS acceleration presented here does not include acceleration due to gravity. In addition to these spectrograms, we plot their time-average PSD in figures 5(b), 6(c), 7(c) to give a sense of the general long-term frequency content.

A spectrogram of the first group of results can be seen in figure 5(a). The three WS trials have been stitched together to form one continuous sample for ease of presentation. In figure 5(a) we can see that the majority of the power in the signal, shown darker, is focused around 12 Hz and does not

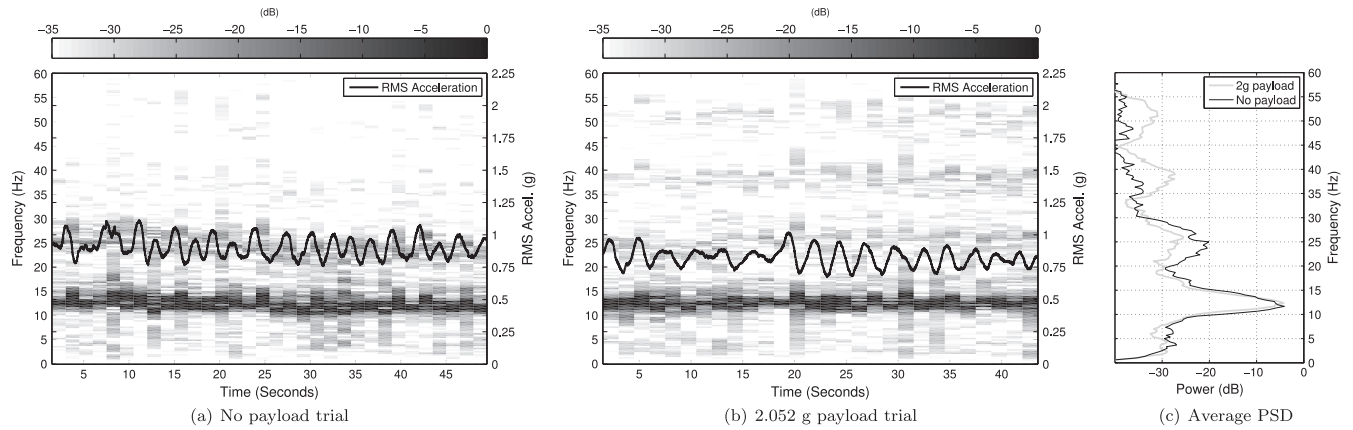


Figure 7. Spectral results of z-component acceleration for thrush 2. Two trials shown highlighting deviations in fundamental frequency when significant payload is attached. Sliding window (1 s) RMS acceleration magnitude plotted on second axis of spectrogram.

seem to vary in time. Small frequency modulations occur between $60 < t < 80$ s, but generally the flapping frequency is consistent. The small shifts that do occur tend to correlate with changes in acceleration magnitude. The second harmonic is visible in this figure as a lighter band near 24 Hz, indicating a higher frequency that could be used for harvester excitation. Despite the approximately 10 dB reduction from the fundamental frequency, the observation is important given the challenges implementing low-frequency, low-mass piezoelectric energy harvesters. The time averaged PSD for this trial shown in figure 5(b) shows that for this bird, there is some broadband frequency content between 12 and 14 Hz, but that there is a peak near 12 Hz.

The results of the first set of thrush trials can be seen in figures 6(a) and (b). These two trials are the results for the same bird, ST1, carrying the same logger and show the types of small variations we might expect in flight from a freely flying bird. Figure 6(a) shows a flapping frequency that starts near 15 Hz for the first 10 s before decreasing slightly, and then increasing back to 15 Hz in the last 4 s of the trial. During the initial portion of this trial, the bird was moving from the rear of the tunnel to the front and thus the frequency variations seen here likely represent the extreme of what might be expected for steady flight. The variation in flapping frequency is evident in the lack of a clear peak in the average PSD for this trial shown 6(c). We can see in this plot that there is significant power for this trial between 12 and 16 Hz with a slight peak near 14 Hz. This can be contrasted against the results for trial two of ST1 in figure 6(b). In this trial, we see a spectrogram that has a series of peaks that appear more constant in time. Additionally, we see that the average PSD for this trial (6(c)) has a peak at 12 Hz. Taken together, these trials suggest that this bird has a fundamental flapping frequency near 12 Hz, but is able to up-regulate its frequency on the order of 25%, consistent with the 20% reported by Hedrick *et al* for cockatiels [9].

The final set of trials compare flights with and without a 2.052 g payload (mass beyond that of the acceleration logger) on ST2 (figure 7). These reveal fundamental frequencies near 12 Hz that do not vary in time. Each of these spectrograms contain data from three individual flights that have been

stitched together. In the flights without payload (figure 7(a)), we see consistent power at 12 Hz with much less power in the second harmonic near 24 Hz. While the fundamental frequency appears nearly identical in the trial with payload (figure 7(b)), there is evidence of more power in the third and fourth harmonics, but less in the second. These results are shown clearly in the average PSDs for these trials shown in figure 7(c). In this figure we see that the bird with and without the 2 g payload had a fundamental frequency of 12 Hz. The changes in the higher harmonics for the payload case indicates that the bird maintains its flapping frequency, but adjusts its flapping gate. The 2.052 g payload, along with the 0.64 g data logger mass represents 6.6% of the mass of the bird, representing 165% the previously mentioned 4% mass limit. Finally, the RMS acceleration between these two trials does not significantly change despite the increase in flown mass. Given these results, it appears safe to assume that payloads do not drastically alter flapping frequencies.

The results of this acceleration testing affirm that the flapping frequency is consistent in time, does not appear to be significantly affected by payloads, and has a significant magnitude of acceleration near 1 g RMS. It is therefore reasonable to assume that knowledge of the unladen flapping frequency is sufficient when designing a resonating energy harvester. The remaining consideration as to the applicability of energy harvesters for this application deals with the specific power of the transduction method.

4. Piezoelectric energy harvesting potential versus power requirements

Previous sections show that there is sufficient energy for harvesting from a flying vertebrate, and the nature of the acceleration lends itself to resonant energy harvesting. To understand the amount of power that might be harvested by a piezoelectric device attached to an animal, we must better understand the relationship between harvester mass, frequency, and power output. The specific power from an energy harvester depends on the design and operating frequency, and thus has been hard to generally quantify for the technology.

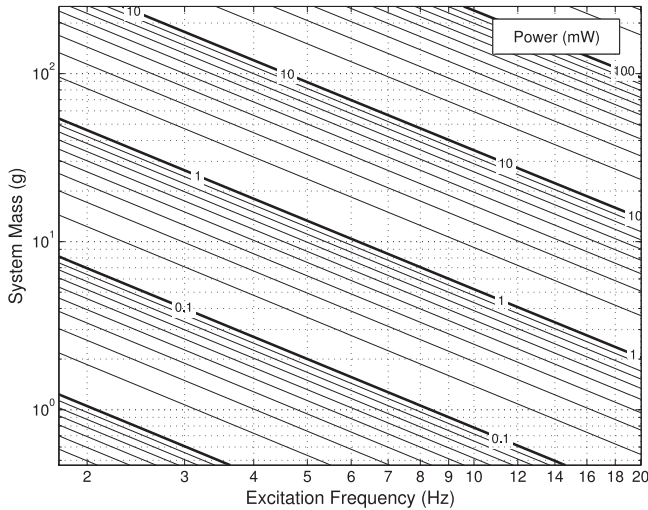


Figure 8. Maximum power available from a fully covered bi-morph piezoelectric vibrational energy harvester based on maximum stress. No factor of safety applied.

Table 1. List of material properties.

	Value	Unit	Name
ρ_s	7916.5	kg m^{-3}	Substrate density
ρ_p	7800	kg m^{-3}	Piezoelectric material density
E_{sx}	212	GPa	Substrate modulus
E_{px}	67	GPa	Piezoelectric material modulus
e	-12.73	C m^{-2}	Piezoelectric stress constant
ϵ^s	1.59e-8	C m^{-2}	Piezoelectric permittivity
σ_{\max}	76	MPa	Piezoelectric ultimate strength

Recently, we proposed a baseline based on optimization of the piezoelectric material thickness ratio and the ultimate strength of the piezoelectric element [30]. We will use this analysis here to estimate specific power.

The power limit for piezoelectric energy harvesters depends on the maximum allowable stress in the device. Based on this and a thickness ratio optimization [34], we developed a set of harvester designs across a range of harvester masses and excitation frequencies. The maximum power reported depends on the material chosen and two geometric parameters relating harvester width to length, and length to mass.

This power limit has been recomputed here for a range of masses and frequencies applicable to many bird and bat species. The results of this analysis are shown in figure 8. This analysis was done for a beam aspect ratio (length/width) of five and a mass constant (mass/length³) of 45.6 kg m^{-3} . The piezoelectric material was Navy Type II and the substrate material was stainless steel, two standard materials for harvesters. The material properties are shown in table 1.

In figure 8, we see that the maximum power for devices on these scales is on the order of milliwatts. There is a dependence on harvester mass. Using the known mass ($\sim 40 \text{ g}$) and flapping frequency (12 Hz) of the tested thrushes as an example, we can use figure 8 to estimate the power. Using the 4% mass limit, a harvester system for this bird should weigh less than 1.6 g. According to figure 8, a 1.6 g

harvester operating at 12 Hz could produce up to $250 \mu\text{W}$. We assume a factor of safety of four, as figure 8 represents power immediately prior to failure. As such, we estimate $62 \mu\text{W}$ of power harvested for this case. This is a significant amount of power when compared to the daily energy requirements of bio-logging device microcontrollers. Excess energy would be stored and used during high power operations.

Table 2 contains a compiled list of power requirements for microcontrollers that could be used on such a system. The devices all require on the order of a few hundred microwatts, with the lowest operating at $180 \mu\text{W}$. The $62 \mu\text{W}$ that we might expect from the Swainson's thrush is not sufficient to directly power these devices at 1 MHz, but the current draw on most microcontrollers is linearly related to the clock frequency. For example, operating the MSP420FR5X series microcontroller at 250 kHz would require $45 \mu\text{W}$, less than what we estimated could be produced. Furthermore, bio-logging tags operate at very low duty cycles and are often in an active power mode for only a few seconds per day. Power harvested when the tag is in a sleep mode would be stored (battery or capacitor) for use during active periods. Given these results, it is evident that even birds as small as a thrush could use a piezoelectric energy harvester to generate sufficient power in flight to operate a bio-logging device.

To further explore the viability of vibrational energy harvesters as a power source for wildlife bio-loggers, we will show the operational requirements necessary to maintain a positive energy budget for an example system applied to a variety of bird species. This example system will be a bio-logging device that takes one sensor measurement per minute for 12 h a day, and downlinks the data once a day. We will assume that each measurement requires 1 byte of memory and requires 10 ms to acquire. Table 3 contains the parameter assumptions for the example data logger explored here.

Based on the assumed power consumption and rate of sampling and transmission, we can develop daily energy requirements with the following equation:

$$E_{\text{out}} = P_{\text{act}}t_{\text{act}} + P_{\text{tx}}t_{\text{tx}} + P_{\text{low}}t_{\text{low}}. \quad (20)$$

Here t_* represents the time per day that the system is in either active/sensing, transmission, or low/time-keeping mode, as defined by:

$$t_{\text{act}} = t_m N_m, \quad (21)$$

$$t_{\text{tx}} = R_{\text{tx}}^{-1} N_m D, \quad (22)$$

$$t_{\text{low}} = t_{\text{day}} - (t_{\text{act}} + t_{\text{tx}}), \quad (23)$$

where t_{day} is one day (86 400 s). Substituting these into equation (20) and rearranging gives

$$E_{\text{out}} = \left[(P_{\text{act}} - P_{\text{low}})t_m + (P_{\text{tx}} - P_{\text{low}})R_{\text{tx}}^{-1}D \right] N_m + P_{\text{low}}t_{\text{day}}. \quad (24)$$

We can compare this expenditure to the daily harvested energy, E_h :

$$E_h = P_{\text{gen}}t_{\text{gen}}\eta_{\text{storage}}, \quad (25)$$

where t_{gen} is the time per day that the harvester is generating

Table 2. Power consumption for microcontroller devices.

Manufacturer	Model	Active@1 MHz (mW)	Low power mode (μ W)
Texas Instruments	MSP430F2XX	0.44	0.22
	MSP430FR5X	0.18	0.18
Atmel Corporation	ATtinyX4A	0.38	0.18
	ATtinyX61/V	0.54	0.18
	ATmega165	0.39	0.18
Microchip	PIC24F16KL402	0.63	0.054
	PIC24FV16KM204 F	0.36	0.045

Table 3. Example bio-logger system parameters.

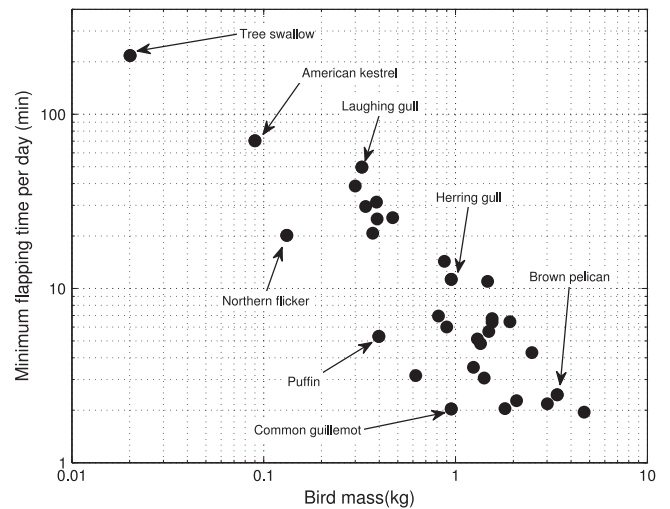
Parameter	Variable name	Assumed value	Units
Power: sensing	P_{act}	300 μ A@3 V	mW
Power: time-keeping	P_{low}	1 μ A@3 V	mW
Power: transmitting	P_{tx}	20 mA@3 V	mW
Measurements/day	N_m	720	#/day
Time/measurement	t_m	10	ms/measurement
Transmissions/day	N_{tx}	1	#/day
Transmission rate	R_{tx}	250	k-bits/s
Data size/measurement	D	1	bytes/measurement

power. Given this and equation (24), we can estimate the amount of active power generation time (flight time) required to maintain a positive energy budget.

$$t_{gen} > \frac{\left[\left[(P_{act} - P_{low})t_m + (P_{tx} - P_{low})R_{tx}^{-1}D \right] N_m + P_{low}t_{day} \right]}{P_{gen}\eta_{storage}}. \quad (26)$$

With this expression and the assumptions made in table 3, we can estimate the daily activity requirements for positive energy budgets. This was carried out for a variety of species with known masses and flapping frequencies [35], as shown in table 4. Equation (26) depends on the power generated by each bird in flight (P_{gen}). We use figure 3(a) to make this estimate, equating harvester power (P_h) to generated power (P_{gen}), but need to know the specific power of the piezoelectric transducer used for each bird under consideration. The results presented in figure 8 can be used to estimate the specific power (\bar{P}) of a harvester sized to approximately 4% of the mass of the bird. This specific power estimate (using a factor of safety of four) has been made for each species in the dataset, and the results are presented in table 4. With these specific power estimates and knowledge of the mass of the birds, we can use figure 3(a) to estimate the amount of safely harvestable power. This too is presented in table 4. With these estimates of harvestable power, we use equation (26) to determine the daily flight time required to maintain positive energy budgets. The results of this calculation are presented in table 4 and figure 9. We assume a storage efficiency ($\eta_{storage}$) of unity based on the high efficiencies of capacitors and rechargeable lithium-ion batteries [36].

In figure 9 we can see that the required amount of flapping activity for a positive energy budget scales with the mass of the bird. As the bird mass decreases, more active time is required per day. Although smaller birds tend to have higher flapping frequencies [37], which would tend to increase

**Figure 9.** Minimum flapping time required to power example bio-logger.

specific power output, figure 9 shows reductions in power from their smaller size dominates this increase. Although smaller birds do tend to require more activity to maintain a positive energy balance, the requirements are still within what would be considered reasonable. The smallest bird considered in this data set was the tree swallow (*Tachycineta bicolor*). Given this example system, this bird would need to be active (flapping) for approximately 3.6 h per day. This required flapping time decreases quickly with increases in bird mass. The American kestrel (*Falco sparverius*) would need 70 min of flapping and a great black-backed gull (*Larus marinus*) would require only 7 min. Even for this relatively capable example bio-logging system, with daily downlinking of data, the activity requirements of the host animals are in a range

Table 4. Avian power generation estimates. Mass and frequency data from [35].

Common name	Latin name	Mass (kg)	Frequency (Hz)	\bar{P} (mW kg ⁻¹)	P_h (mW)	Minimum t_{act} (min)
Puffin	<i>Fratercula arctica</i>	0.398	9.18	53	0.84	5
Common guillemot	<i>Uria aalge</i>	0.95	8.69	58	2.19	2
Razorbill	<i>Alca torda</i>	0.62	9.08	57	1.41	3
Great skua	<i>Catharacta skua</i>	1.35	3.93	17	0.92	5
Arctic skua	<i>Stercorarius parasiticus</i>	0.39	3.61	11	0.18	25
Kittiwake	<i>Rissa tridactyla</i>	0.387	3.18	9	0.14	31
Great black-backed gull	<i>Larus marinus</i>	1.55	2.90	11	0.66	7
Herring gull	<i>Larus argentatus</i>	0.95	3.05	10	0.39	11
Laughing gull	<i>Larus atricilla</i>	0.325	2.74	7	0.09	50
Royal tern	<i>Sterna maxima</i>	0.47	3.12	9	0.17	25
Black skimmer	<i>Rynchops niger</i>	0.3	3.36	10	0.12	39
Fulmar	<i>Fulmarus glacialis</i>	0.815	4.58	20	0.64	7
White-tailed tropicbird	<i>Phaethon lepturus</i>	0.37	4.22	15	0.21	21
Northern gannet	<i>Sula bassanus</i>	3.01	3.53	17	2.04	2
Anhinga	<i>Anhinga anhinga</i>	1.24	5.07	25	1.26	4
Double-crested cormorant	<i>Phalacrocorax auritus</i>	1.41	5.03	26	1.45	3
Shag	<i>Phalacrocorax aristotelis</i>	1.81	5.35	30	2.18	2
Brown pelican	<i>Pelecanus occidentalis</i>	3.39	3.01	13	1.81	2
Magnificent frigatebird	<i>Fregata magnificens</i>	1.47	2.24	7	0.41	11
Roseate spoonbill	<i>Ajaia ajaja</i>	1.3	3.90	17	0.87	5
White ibis	<i>Eudocimus albus</i>	0.9	4.65	21	0.74	6
Great white heron	<i>Ardea occidentalis</i>	2.5	2.68	10	1.04	4
Great blue heron	<i>Ardea herodias</i>	1.92	2.55	9	0.69	6
Great egret	<i>Casmerodius albus</i>	0.874	2.79	9	0.31	14
Little blue heron	<i>Egretta caerulea</i>	0.34	3.63	11	0.15	30
Turkey vulture	<i>Cathartes aura</i>	1.55	2.99	11	0.69	6
Black vulture	<i>Coragyps atratus</i>	2.08	4.53	24	1.96	2
Bald eagle	<i>Haliaeetus leucocephalus</i>	4.68	2.72	12	2.28	2
American kestrel	<i>Falco sparverius</i>	0.09	5.70	18	0.06	70
Osprey	<i>Pandion haliaetus</i>	1.49	3.31	13	0.79	6
Northern flicker	<i>Colaptes auratus</i>	0.132	9.19	42	0.22	20
Tree swallow	<i>Tachycineta bicolor</i>	0.0201	8.72	26	0.02	217

that make piezoelectric harvesting a viable option for power generation.

5. Conclusion

With reductions in the power consumption of microelectronic components and the advent of piezoelectric vibrational energy harvesting, electrical systems powered using ambient vibrations are now possible. We have shown that the use of vibrational energy harvesting in the realm of wildlife computing is not only possible, but appears to be an advantageous method of energy production in applications involving a broad range of bird and bat species. Not only is there theoretically enough power available from most bird species to power a bio-logging device, but there is a transduction method capable of harnessing that energy. The need for standard piezoelectric devices to operate at a specific resonant frequency appears to be matched well to the accelerations expected for bird flight. Moreover, even while considering the payload limitations for flying

vertebrates, piezoelectric devices could be designed to harvest a significant amount of power. We have shown that even when the harvester power is reduced by a factor of safety of four, there would still be sufficient power generated to warrant their use. Furthermore, for most species, a typical bio-logger powered using a piezoelectric harvester could operate with positive energy budgets while requiring only modest activity from its host. This evidence suggests that vibrational energy harvesting should be considered as a power source for future wildlife bio-logging devices, and that future work is needed in this area to implement the concepts presented here.

Acknowledgments

This research was supported by NSF grant CMMI-1014891 and NSF Graduate Research Fellowship Program grant DGE0707428. The authors would like to thank Wayne Bezner-Kerr for his help during the bird flight experiments.

Appendix A. Avian power model

Table A1. Power types and equations for bird flight [25].

Power type	Description	Equation
Parasitic (P_{par})	Drag from body	$1/2\rho V^3 S_b C_{\text{Db}}$
Induced (P_{ind})	Momentum transfer to air (lift)	$\frac{km^2 g^2}{2S_d V\rho}$
Profile (P_{pro})	Driving wings forward through flow	$\frac{C_{\text{pro}} 1.05k^{3/4} m^{3/2} g^{3/2} S_b^{1/4} C_{\text{Db}}^{1/4}}{A_R \rho^{1/2} B^{3/2}}$
Basal metabolic (P_{M})	Caloric overhead	$\eta\alpha m^\delta$
Cardio/pulmonary	Cardiovascular/breathing	$0.1(P_{\text{par}} + P_{\text{ind}} + P_{\text{pro}} + P_{\text{M}})$

Table A2. Bird flight power model nomenclature and constants [25, 29].

Name	Variable	Constants
Wing aspect ratio	A_R	
Wingspan	B	
Profile power constant-empirical	C_{pro}	8.4
Body drag coefficient	C_{Db}	0.1
Harvester specific power	\bar{P}	
Maximum harvestable power	P_{H}	
Harvestable power	P_{h}	
Induced power	P_{ind}	
Laden power output	P_{l}	
Metabolic power output	P_{M}	
Parasitic drag power	P_{par}	
Profile power	P_{pro}	
Body frontal area	S_b	$8.13 \times 10^{-3} m^{0.666}$
Circular area swept by wings	S_d	
Forward flight velocity	V	
Acceleration due to gravity	g	
Induced drag factor-empirical	k	0.9
Mass of bird (unladen)	m	
Total laden mass (payload and energy harvester)	m_{l}	
Payload mass (other than energy harvester)	m_{p}	
Allowable fraction of laden mass (3–4%)	q	
Metabolic mass constant	α	$\begin{cases} 6.25 & \text{for passerines} \\ 3.79 & \text{for non-passerines} \end{cases}$
Metabolic conversion efficiency	η	
Metabolic mass exponent	δ	$\begin{cases} 0.724 & \text{for passerines} \\ 0.723 & \text{for non-passerines} \end{cases}$
Air density	ρ	

Appendix B. Quartic solution variables

The solution to the quartic polynomial

$$Ax^4 + Bx^3 + Cx^2 + Dx + E = 0 \quad (\text{B.1})$$

has the following solution

$$x = \frac{-B}{4A} + \frac{\pm_i W \mp_j \sqrt{-(3\lambda + 2y \pm \frac{2\beta}{iW})}}{2}, \quad (\text{B.2})$$

where

$$\lambda = \frac{-3B^2}{8A^2} + \frac{C}{A},$$

$$\beta = \frac{B^3}{8A^3} - \frac{BC}{2A^2} + \frac{D}{A},$$

$$\gamma = \frac{-3B^4}{256A^4} + \frac{CB^2}{16A^3} - \frac{BD}{4A^2} + \frac{E}{A},$$

$$P = \frac{-\lambda^2}{12} - \gamma,$$

$$Q = \frac{-\lambda^3}{108} + \frac{\lambda\gamma}{3} - \frac{\beta^2}{8},$$

$$R = \frac{-Q}{2} + \sqrt{Q^2/4 + P^3/27},$$

$$U = R^{1/3},$$

$$y = \begin{cases} -\frac{5}{6}\lambda - Q^{1/3} & \text{if } U = 0, \\ -\frac{5}{6}\lambda + U - \frac{P}{3U} & \text{if } U \neq 0, \end{cases}$$

$$W = \sqrt{\lambda + 2y},$$

References

- [1] Patton D R, Beaty D W and Smith R H 1973 Solar panels: an energy source for radio transmitters on wildlife *J. Wildlife Manage.* **37** 236–8
- [2] Microwave Telemetry Inc 2013 PTT-100 5 gram solar PTT Retrieved from http://www.microwavetelemetry.com/bird/solarPTT_5g.cfm
- [3] Microwave Telemetry Inc 2013 Battery powered Argos/GPS LC4™ PTT-100 s Retrieved from <http://microwavetelemetry.com/bird/batteryArgosGPS.cfm>
- [4] MacCurdy R, Reissman T, Garcia E and Winkler D 2008 A methodology for applying energy harvesting to extend wildlife tag lifetime *Proc. ASME 2008 Conf. of Smart Materials Adaptive Structures Intelligent Systems*, number 48692 (ASME) pp 121–30
- [5] Wickenheiser A and Garcia E 2010 Power optimization of vibration energy harvesters utilizing passive and active circuits *J. Intell. Mater. Syst. Struct.* **21** 1343–61
- [6] Shu Y C and Lien I C 2006 Analysis of power output for piezoelectric energy harvesting systems *Smart Mater. Struct.* **15** 1499–512
- [7] Reissman T, MacCurdy R B and Garcia E 2011 Electrical power generation from insect flight *SPIE Smart Structures and Materials + Nondestructive Evaluation and Health*

- Monitoring* (International Society for Optics and Photonics) p 797702
- [8] Aktakka E E, Kim H and Najafi K 2011 Energy scavenging from insect flight *J. Micromech. Microeng.* **21** 095016
- [9] Hedrick T L, Tobalske B W and Biewener A A 2003 How cockatiels (*nymphicus hollandicus*) modulate pectoralis power output across flight speeds *J. Exp. Biol.* **206** 1363–78
- [10] Bullen R D and McKenzie N L 2002 Scaling bat wingbeat frequency and amplitude *J. Exp. Biol.* **205** 2615–26
- [11] Shafer M W and Garcia E 2011 Maximum and practical sustainably harvestable vibrational power from avian subjects *Proc. ASME 2011 Conf. of Smart Materials Adaptive Structures Intelligent Systems, number 54723* (ASME) pp 353–9
- [12] Shafer M W, MacCurdy R, Garcia E and Winkler D 2012 Harvestable vibrational energy from avian sources: theoretical predictions versus measured values *SPIE Smart Structures and Materials + Nondestructive Evaluation and Health Monitoring, number 834103* 11–15 March 2012 (International Society for Optics and Photonics)
- [13] Pennycuick C J 1969 The mechanics of bird migration *Ibis* **111** 525–56
- [14] Pennycuick C J, Farner D S, King J R and Parkes K C 1975 *Avian Biology: Mechanics of Flight* vol 5 (New York: Academic)
- [15] Pennycuick C J, Obrecht H H and Fuller M R 1988 Empirical estimates of body drag of large waterfowl and raptors *J. Exp. Biol.* **135** 253–64
- [16] Norberg U M L and Norberg R Å 2012 Scaling of wingbeat frequency with body mass in bats and limits to maximum bat size *J. Exp. Biol.* **215** 711–22
- [17] Marden J H 1987 Maximum lift production during takeoff in flying animals *J. Exp. Biol.* **130** 235–58
- [18] Vandenabeele S P, Shepard E L, Grogan A and Wilson R P 2012 When three per cent may not be three per cent; device-equipped seabirds experience variable flight constraints *Mar. Biol.* **159** 1–14
- [19] USGS 2011 How to request auxiliary marking permission Retrieved from <http://pwrc.usgs.gov/bbl/manual/aarequs.cfm>
- [20] Neubaum D J, Neubaum M A, Ellison L E and O'Shea T J 2005 Survival and condition of big brown bats (*eptesicus fuscus*) after radiotagging *J. Mammalogy* **86** 95–98
- [21] Hill D A and Robertson P A 1987 The role of radio-telemetry in the study of galliformes *World Pheasant Assoc. J.* **12** 81–92
- [22] Hedin R S and Caccamise D F 1982 A method for selecting transmitter weights based on energetic cost of flight *Trans. Northeast Fish and Wildlife Conf.* vol 39 p 115
- [23] Naef-Daenzer B, Widmer F and Nuber M 2001 A test for effects of radio-tagging on survival and movements of small birds *Avian Sci.* **1** 15–23
- [24] Bontadina F, Schofield H and Naef-Daenzer B 2002 Radio-tracking reveals that lesser horseshoe bats (*rhinolophus hipposideros*) forage in woodland *J. Zoology* **258** 281–90
- [25] Pennycuick C J 2008 *Modeling the Flying Bird* (New York: Academic)
- [26] Poole E L 1938 Weights and wing areas in North American birds *Auk* **55** 511–7
- [27] Cornell Lab of Ornithology 2011 All about birds <http://www.allaboutbirds.org/Page.aspx?pid=1189>
- [28] Pennycuick C J 1997 Actual and 'optimum' flight speeds: field data reassessed *J. Exp. Biol.* **200** 2355–61
- [29] Pennycuick C J, Åkesson S and Hedenström A 2013 Air speeds of migrating birds observed by ornithodolite and compared with predictions from flight theory *J. R. Soc. Interface* **10** 20130419
- [30] Shafer M W and Garcia E 2014 The power and efficiency limits of piezoelectric energy harvesting *J. Vib. Acoust.* **136** 021007
- [31] Borgeson J 2012 Ultra-low-power pioneers: Ti slashes total mcu power by 50 percent with new 'wolverine' mcu platform *White paper, Texas Instruments* Post Office Box 655303, Dallas, Texas 75265
- [32] Gerson A R and Guglielmo C G 2011 Flight at low ambient humidity increases protein catabolism in migratory birds *Science* **333** 1434–6
- [33] Rappole J H and Tipton A R 1991 New harness design for attachment of radio transmitters to small passerines *J. Field Ornithology* **62** 335–7
- [34] Shafer M W, Bryant M and Garcia E 2012 Designing maximum power output into piezoelectric energy harvesters *Smart Mater. Struct.* **21** 085008
- [35] Pennycuick C J 1990 Predicting wingbeat frequency and wavelength of birds *J. Exp. Biol.* **150** 171–85
- [36] Ohzuku T, Ueda A, Yamamoto N and Iwakoshi Y 1995 Factor affecting the capacity retention of lithium-ion cells *J. Power Sources* **54** 99–102
- [37] Pennycuick C J, Klaassen M, Kvist A and Lindstrom A 1996 Wingbeat frequency and the body drag anomaly: wind-tunnel observations on a thrush nightingale (*luscinia luscinia*) and a teal (*anas crecca*) *J. Exp. Biol.* **199** 2757–65